Analysis of the absorption spectrum of neodymium:sodium beta double prime alumina

A. J. Alfrey, O. M. Stafsudd, B. Dunn, and D. L. Yang

Citation: The Journal of Chemical Physics **88**, 707 (1988); doi: 10.1063/1.454149
View online: http://dx.doi.org/10.1063/1.454149
View Table of Contents: http://scitation.aip.org/content/aip/journal/jcp/88/2?ver=pdfcov
Published by the AIP Publishing

Analysis of the absorption spectrum of neodymium:sodium beta double prime alumina

A. J. Alfrey and O. M. Stafsudd
Department of Electrical Engineering, University of California, Los Angeles, Los Angeles, California 90024
B. Dunn and D. L. Yang
Department of Materials Science, University of California, Los Angeles, Los Angeles, California 90024

(Received 6 July 1987; accepted 1 October 1987)

The Judd–Ofelt analysis has been applied to the sigma-polarized absorption spectrum of Nd^{3+}:NaB″alumina to determine the modified Judd–Ofelt parameters $\Omega_{\sigma,2}$, $\Omega_{\sigma,4}$, and $\Omega_{\sigma,6}$. A model for the near-neighbor environment of Nd^{3+} has been proposed and tested using a simplified point charge model for the crystal field. The model indicates that the observed spectrum may be explained by a large linear field term in the crystal field induced by the shift in position of conduction plane oxygen and neodymium ions away from sites of inversion symmetry.

I. INTRODUCTION

Recent work has described how optically active trivalent transition metal and rare earth ions can be substituted for monovalent Na^+ in sodium beta double prime alumina (SB″A) by using low-temperature exchange processes.[1,2] Jansen *et al.*[3] used this approach to prepare small platelets of various exchange percentages and observed laser action at 1.06 μ in some of them. In addition, they reported the existence of an anomalously strong absorption line at 5800 Å similar to the so-called hypersensitive line observed in other rare-earth/host systems.[4] In the present paper, we provide a more detailed examination of the sigma-polarized absorption spectra for samples of Nd^{3+}:SB″A by performing a modified Judd–Ofelt analysis.[5,6] The Judd–Ofelt analysis is typically used to derive three phenomenological parameters useful for comparing the oscillator strengths and predicting the emission cross sections for the rare earths in glass and crystalline environments. In its original formulation, the analysis was applied to active ions within isotropic environments. However, when applied to anisotropic uniaxial[7] and biaxial[8] crystals, both pi and sigma polarized absorption spectra have been required to synthesize the Judd–Ofelt parameters. In the current work, the platelet structure of the SB″A crystals has made it difficult to obtain pi polarized spectra by propagating light edgewise through the crystals. Therefore, we have experimentally determined Judd–Ofelt parameters for sigma-polarized spectra only and have derived a theoretical form for sigma and pi polarized Judd–Ofelt parameters that, like the isotropic version, depend on the odd-order crystal field parameters. Finally, we have calculated theoretical values for the pi and sigma polarized parameters based on a simple point charge model for the nearest-neighbor environment of the Nd^{3+} ion made available from x-ray diffraction work. Because of the high mobility of some ions in the conduction plane of SB″A, we may treat their positions as adjustable parameters and thereby calculate Judd–Ofelt parameters as a function of crystal field ion position.

II. CRYSTAL STRUCTURE OF SB″A AND Nd:SB″A

The structure of SB″A has been reviewed by several authors[9,11] and we will discuss only those characteristics of immediate importance to the current work. The structure consists of spinel blocks of closely packed Al^{3+} and O^{2-} separated by loosely packed slabs containing Na^+ and O^{2-}. The open space in these slabs permits rapid Na^+ migration in two dimensions (in a plane perpendicular to the "*c*" axis). Figure 1 shows the result of projecting the conduction slab ions onto the mid-plane, or so-called conduction plane. In a typical composition of $Na_{1.67}Mg_{0.67}Al_{10.33}O_{17}$, where Mg substitutes for Al in the spinel blocks during the raw crystal growth to stabilize the "beta" phase, Na^+ ions occupy $\frac{5}{6}$ of two crystallographically equivalent sites (Beevers–Ross and anti-Beevers–Ross sites) whose positions are denoted 6*c* sites in the Wyckoff notation in the $R\bar{3}m$ point group.[10] These positions are alternately shifted slightly up and down from the midplane. Trivalent rare earths may be diffused into the conduction plane and substituted for Na^+, leaving the spinel blocks unchanged. Exchange percentages typical-

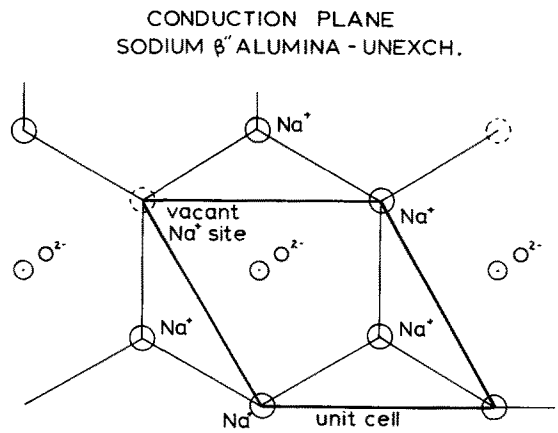

FIG. 1. Conduction plane of unexchanged sodium beta double prime alumina.

 0021-9606/88/020707-10$02.10

ly range from 20% of all Na^+ ions exchanged to over 95% exchange, corresponding to Nd^{3+} ion concentrations of 3.6×10^{20} to 1.8×10^{21} cm^{-3}, respectively. The raw crystals for the current work were grown by isothermal flux evaporation as per the procedure outlined by Roth *et al.*[11] The ion exchange technique is as described by Farrington and Dunn[2] and as described in the current work in Sec. IV.

Recent x-ray diffraction work[8] has shown that, when gadolinium is totally exchanged for sodium, gadolinium preferentially occupies mid-oxygen sites as shown in Fig. 2, with a small percentage of unit cells found to contain gadolinium at the Beevers–Ross sites. Soon-to-be published work[12] indicates essentially the same site occupation for Nd^{3+}. Referring to the work of Carrillo–Cabrera *et al.*, we display the nearest-neighbor structure of fully exchanged Gd:SB″A, where we have used the same labels as the authors to label ion positions.[10] The rare-earth ion occupies a so-called mid-oxygen site [labeled Gd(2) and occupying a Wyckoff position 9*d*] situated between oxygen ions in the plane [labeled O(5), Wyckoff position 18*g*] and between oxygen ions above and below the plane within the spinel blocks [labeled O(4) and O(3), Wyckoff positions 18*h* and 6*c*, respectively, with both O(3) and O(4) sites in each spinel block]. We further note that Fourier synthesis maps indicate that not only are the mid-plane O^{2-} distorted towards the mid-oxygen positions by ~0.5 Å but the Gd^{3+} position is also found to be distributed in elliptical fashion over several tenths of angstroms. The work of Thomas[12] indicates that similar distortions are present in partially exchanged Nd:SB″A except that the mid-plane oxygen ions are distorted in a diagonal direction toward Beevers–Ross and anti-Beevers–Ross sites. Since Fourier maps average over many unit cells, individual distortions are not visible and the maps indicate that distortions toward all Beevers–Ross sites are allowed. In actuality, the sites to which particular oxygen ions are distorted are determined by the sodium exchange conditions at each unit cell. It will be shown in Secs. VI and VII that such distortions are essential to the potential understanding of the absorption spectrum of Nd:SB″A and that a particular form of asymmetry in this distortion is required to yield the observed optical spectra.

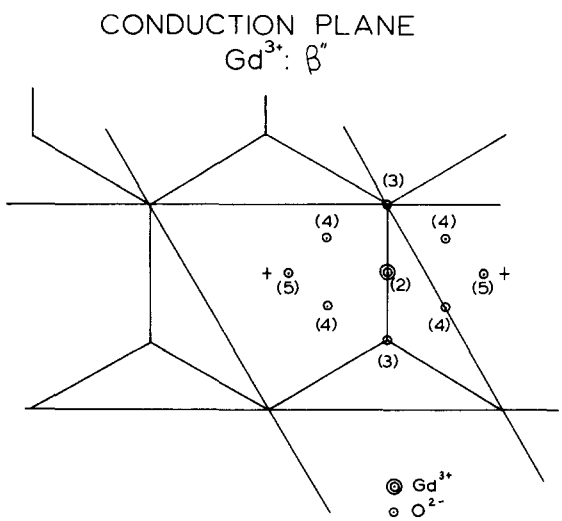

FIG. 2. Conduction plane for totally exchanged Gd^{3+}:SB″A.

III. JUDD–OFELT THEORY

The Judd–Ofelt theory[5] is traditionally used to account for the presence of parity-forbidden electric dipole transitions for rare-earth ions in crystalline and glass hosts.[13,14] In this model, the near-neighbor crystal field is responsible for the admixture of odd-parity configurations into the $4f^n$ configuration. This theory is particularly successful for isotropic materials such as Nd:glass, in which the oscillator strength of absorption transitions between the Stark-split ground state $|i\rangle$ and the excited state $|f\rangle$ is given by

$$P=\sum_{\substack{\text{even}\\ \lambda}} \nu\, T_\lambda |\langle i\|U^{(\lambda)}\|f\rangle|^2, \tag{1}$$

where T_λ are parameters dependent on radial integrals, $3-J$ and $6-J$ symbols, and crystal field parameters, and where $\langle i\|U^{(\lambda)}\|f\rangle$ are reduced matrix elements. For anisotropic materials such as the uniaxial SB″A, we must modify the expression slightly to account for pi and sigma polarizations.

From the work of Judd,[5] we start with the expression [Judd, Eq. (1)] for the oscillator strength of a dipole transition between states $|i\rangle$ and $|f\rangle$:

$$P_q = X\frac{8\pi^2 m\nu}{h}|\langle i|D_q^{(1)}|f\rangle|^2, \tag{2}$$

where $X=(n^2+2)^2/9n$, the correction for the polarizability of the host,

$$D_q^{(k)}=\sum_{\substack{j\text{th}\\ \text{electron}}} r_j^k\, C_q^{(k)}(\theta_j,\phi_j) \tag{3}$$

and

$$C_q^{(k)}(\theta_j,\theta_j)=\left(\frac{4\pi}{2k+1}\right)Y_{kq}(\theta_j,\phi_j). \tag{4}$$

The choice of $q=\pm1$ corresponds to sigma polarization and $q=0$ corresponds to pi polarization.

The matrix element for the dipole moment operator is given by [Judd, Eq. (13)]

$$\begin{aligned}\langle i|D_q^{(1)}|f\rangle &= \sum_{p,t,M,M'}(2\lambda+1)(-1)^{p+q}A_{t,p}\begin{pmatrix}1 & \lambda & t\\ q & -p-q & p\end{pmatrix}\\ &\quad\times\langle 4f^n\psi JM|U^{\lambda}_{p+q}|4f^n\psi' J'M'\rangle\Xi(t,\lambda),\end{aligned} \tag{5}$$

where

$$\begin{aligned}\Xi(t,\lambda) &= 2\sum_{n'l'}(2l+1)(2l'+1)(-1)^{l+l'}\\ &\quad\times\begin{Bmatrix}1 & \lambda & t\\ l & l' & l\end{Bmatrix}\begin{pmatrix}l & 1 & l'\\ 0 & 0 & 0\end{pmatrix}\begin{pmatrix}l' & t & l\\ 0 & 0 & 0\end{pmatrix}\\ &\quad\times\frac{\langle nl|r|n'l'\rangle\langle nl|r^t|n'l'\rangle}{\Delta(n'l')}.\end{aligned} \tag{6}$$

At this point, a summation is usually performed over Stark levels M and M' and, for isotropic materials, a factor of 1/3 is included along with a summation over q to account for the random orientation of the atomic dipoles, resulting in Eq.

(1) of this paper, in which

$$T_\lambda = \frac{X\,8\pi^2 m(2\lambda+1)}{3h(2J+1)} \sum_t \frac{\Xi^2(t,\lambda)}{(2t+1)} \sum_p |A_{tp}|^2. \quad (7)$$

However, we wish to maintain the polarization dependence, so we substitute Eq. (5) into Eq. (2) and expand the result to yield

$$|\langle i|D_q^{(1)}|f\rangle|^2 = \sum_{pt\lambda} (2\lambda+1)(-1)^{p+q} A_{tp}^* \begin{pmatrix} 1 & \lambda & t \\ q & -p-q & p \end{pmatrix} \langle 4f^n\psi JM|U^\lambda_{p+q}|4f^n\psi' J'N'\rangle$$
$$\times \Xi(t,\lambda) \sum_{\tilde{p}\tilde{t}\tilde{\lambda}} (2\tilde{\lambda}+1)(-1)^{\tilde{p}+q} A_{\tilde{t}\tilde{p}} \begin{pmatrix} 1 & \tilde{\lambda} & \tilde{t} \\ q & -\tilde{p}+q & \tilde{p} \end{pmatrix} \langle 4f^n\psi JM|U^{\tilde{\lambda}}_{\tilde{p}+q}|4f^n\psi' J'M'\rangle \Xi(\tilde{t},\tilde{\lambda}). \quad (8)$$

Applying the Wigner–Eckhart theorem to each matrix element results in the substitutions

$$\langle JM|U^\lambda_{p+q}|J'M'\rangle = (-1)^{J-M} \langle J\|U^\lambda\|J'\rangle \begin{pmatrix} J & \lambda & J' \\ -M & p+q & M' \end{pmatrix} \quad (9)$$

and

$$\langle JM|U^{\tilde{\lambda}}_{\tilde{p}+q}|J'M'\rangle = (-1)^{J-M} \langle J\|U^{\tilde{\lambda}}\|J'\rangle \begin{pmatrix} J & \tilde{\lambda} & J' \\ -M & \tilde{p}+q & M' \end{pmatrix}. \quad (10)$$

Since $J-M$ is an integer, the factor $(-1)^{J-M} \times (-1)^{J-M} = 1$. Since the only dependence on M and M' is in the $3-J$ symbols and the reduced matrix elements, when the summation over M and M' is performed we will be concerned with the evaluation of the product

$$(-1)^{2J+2J'+\lambda+\tilde{\lambda}} \langle J\|U^\lambda\|J'\rangle\langle J\|U^{\tilde{\lambda}}\|J'\rangle \times \sum_{MM'} \begin{pmatrix} J & J' & \lambda \\ -M & M' & p+q \end{pmatrix} \begin{pmatrix} J & J' & \tilde{\lambda} \\ -M & M' & \tilde{p}+q \end{pmatrix}. \quad (11)$$

The normalization of the 3-J symbols

$$\sum_{MM'} \begin{pmatrix} J & J' & \lambda \\ -M & M' & p+q \end{pmatrix} \begin{pmatrix} J & J' & \tilde{\lambda} \\ -M & M' & \tilde{p}+q \end{pmatrix} = \frac{1}{(2\lambda+1)} \delta_{\lambda,\tilde{\lambda}}\, \delta_{\tilde{p}+q,p+q} \quad (12)$$

then allows the simplification of Eq. (2) for the oscillator strength to

$$P_q = \sum_{\lambda=2,4,6} \nu T_{\lambda q} |\langle 4f^n\psi J\|U^{(\lambda)}\|4f^n\psi J'\rangle|^2, \quad (13)$$

where

$$T_{\lambda q} = \frac{X\,8\pi^2 m(2\lambda+1)}{n(2J+1)} \sum_{p,t,\tilde{t}} A_{tp}^*\, A_{\tilde{t}p}\, \Xi(t,\lambda)\, \Xi(\tilde{t},\lambda) \times \begin{pmatrix} 1 & \lambda & t \\ q & -p-q & p \end{pmatrix} \begin{pmatrix} 1 & \lambda & \tilde{t} \\ q & -p-q & p \end{pmatrix}, \quad (14)$$

where we have included the $(2J+1)$ Stark multiplicity of the ground state. In keeping with the convention adopted by Krupke,[15] and to assist in comparison with other work, we will express the oscillator strengths in terms of $\Omega_{\lambda,q}$ parameters, where

$$\Omega_{\lambda,q} = \sum_{t,\tilde{t},p} \frac{(2\lambda+1)}{(2t+1)} A_{tp}^*\, A_{\tilde{t}p}\, \Xi(t,\lambda)\, \Xi(\tilde{t},\lambda) \times \begin{pmatrix} 1 & \lambda & t \\ q & -p-q & p \end{pmatrix} \begin{pmatrix} 1 & \lambda & \tilde{t} \\ q & -p-q & p \end{pmatrix} \quad (15)$$

and

$$P_q = \frac{X\,8\pi^2 m\nu}{(2J+1)h} \sum_\lambda \Omega_{\lambda,q}\, |\langle J\|U^\lambda\|J'\rangle|^2. \quad (16)$$

The oscillator strength of an absorption transition is related to the integrated area under a plot of transmitted intensity vs frequency as given by the expression

$$\int \ln \frac{I}{I_0}\, d\nu = \frac{\pi e^2 N l}{cm} P, \quad (17)$$

where N equals the rare-earth ion density in $1/\text{cm}^3$ and l equals the sample length in centimeters.

Since the wavelength may be considered constant over the linewidth, the integral over frequency may be replaced by the integral over wavelength, resulting in the expression

$$\frac{2.3c}{\lambda^2} \int \log \frac{I}{I_0}\, d\lambda = \frac{\pi e^2 N l}{cm} P. \quad (18)$$

Therefore, by taking absorption spectra under pi and sigma polarization, oscillator strengths for each transition may be measured experimentally. By using Eq. (16), a least-squares fitting may be performed and values of $T_{\lambda,q}$ or $\Omega_{\lambda,q}$ may be determined. Finally, theoretical values for T or Ω parameters may be calculated from the crystal field parameters $A_{t,p}$ derived from a point charge or more complex model. The results of the least square fitting are presented in Sec. V and the results of the theoretical calculations presented in Secs. VII and VIII.

IV. PREPARATION OF THE SAMPLES

All of the samples used in this work were provided by the Materials Science Group lead by Professor B. Dunn of the Materials Science Department of the UCLA School of Engineering. Ion exchange was performed in raw crystals first provided by R. Farrington at the University of Pennsylvania and then using crystals grown by L. Salmon of the group at UCLA. The exchange process begins with a raw single crystal of SB″A typically with dimensions of a few millimeters on a side and thickness between 0.1 and 1.0 mm with most of the samples having a thickness of about 0.3 mm. The objective is to diffuse Nd^{3+} ions into the crystal from a melt of $NdCl_3$. However, because $NdCl_3$ is extremely hy-

groscopic, the material must be dried thoroughly before use to prevent oxidization of the chloride upon heating which, in turn, prevents the formation of a uniform melt. Therefore, the $NdCl_3$ must be carefully dried in vacuum at 50–60 deg C for 12 h. At this point, a uniform mix of $NdCl_3$ and NaCl is prepared with the desired molar percentage of Na and Nd (for example, a molar mix 45:55 for $NdCl_3$:NaCl yields samples with a Nd^{3+} concentration of about 8×10^{20} cm^{-3}). The mix is placed in an alumina crucible within a quartz retort and slowly heated to melting within a N_2/Cl flowing atmosphere. After a melt is achieved, the raw crystal, suspended within a quartz sieve, is immersed into the melt for ~1 h after which the crystal is removed, cooled, and washed in water and dilute HCl. Nd^{3+} concentration is obtained by measuring the weight gain of the sample. Typical weight gains are 5–10 mg with an experimental accuracy of 0.1 mg. Therefore, unless the samples chip or disintegrate in the exchange process, Nd^{3+} concentrations are determined to within 10%.

V. SPECTRA AND Ω PARAMETERS FOR Nd:SB″A

Figure 3 shows a typical absorption spectrum for sigma polarization taken at room temperature for a sample of Nd:SB″A with a concentration of $5\times10^{20}/cm^3$ and a thickness of 0.30 mm, using a Cary model 14 spectrophotometer. Structure at wavelengths longer than 700 nm is not displayed in Fig. 3 in the interest of brevity, yet oscillator strengths for the longer wavelength bands are qualitatively similar to those of Nd:YAG. Spectra can also be taken at 77 K with the use of a liquid nitrogen dewar positioned in the sample beam or samples may be measured at temperatures up to 400 °C by the use of a simple heater element. In a subsequent paper, results for pi polarization will also be available. Pi polarized spectra requires propagation through the sample in a direction perpendicular to the *c* axis. Since the crystals are available in the form of small platelets with a thickness of several hundred microns in the direction of the *c* axis and an area of several square millimeters perpendicular to the *c* axis, it is difficult to propagate light through the small cross section afforded by the platelet structure without resorting to waveguiding. A new spectrophotometer based on a computer interfaced dye laser has recently been constructed in our lab and will allow a narrow beam to be propagated edgewise through the platelet.

Comparison with the spectra of Nd^{3+} in other crystalline hosts will qualitatively show that the spectra of Nd:SB″A is inhomogeneously broadened, consistent with the possibility of different near-neighbor environments from unit cell to unit caused by doping-induced strain, variations in the residual sodium population due to defects and variations in the rare-earth ion distribution.

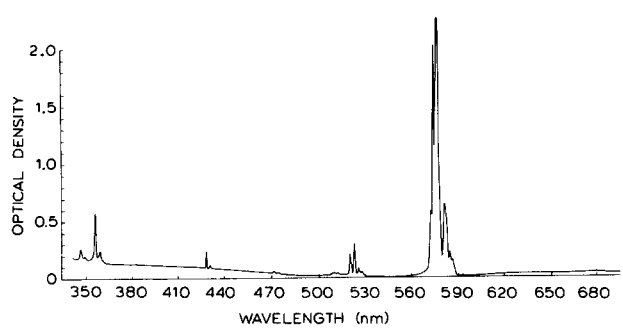

FIG. 3. Absorption spectrum for Nd^{3+}:SB″A with a Nd^{3+} ion concentration of 5×10^{20} cm^{-3}.

TABLE I. Oscillator strengths ($\times10^{-6}$).

Levels	Wavelength (Å)	$NdCl_3$	Nd:YAG	Nd:SB″A
$^4D_{3/2}$,$^2I_{11/2}$,$^4D_{5/2}$, $^4D_{1/2}$,$^2L_{15/2}$	3550	9.52	9.7	13.0
$^2P_{3/2}$	3800	0.05	0.070	
$^2D_{5/2}$	4188	0.08	0.088	
$^2P_{1/2}$	4320	0.38	0.33	0.51
$^2K_{15/2}$,$^2D_{3/2}$,$^2G_{9/2}$, $^4G_{11/2}$	4686	2.31	1.74	0.38
$^2K_{13/2}$,$^4G_{7/2}$,$^4G_{9/2}$	5171	6.58	6.20	6.6
$^2G_{7/2}$,$^4G_{5/2}$	5760	10.5	7.06	47.9
$^2H_{11/2}$	6256	0.39	0.16	
$^4F_{9/2}$	6710	0.83	0.77	
$^4F_{7/2}$,$^4S_{3/2}$	7390	8.88	8.1	4.7
$^4F_{5/2}$,$^2H_{9/2}$	7930	9.22	8.3	4.5
$^4F_{3/2}$	8678	3.02	1.5	1.3

The areas under each curve of transmitted intensity vs wavelength are measured with a K & E polar planimeter and the results of the calculations displayed in Table I for a sample of concentration $5\times10^{20}/cm^3$. Also included in Table I are the oscillator strengths for Nd^{3+} in chloride solutions[5] and for Nd^{3+} in YAG.[15] The wavelengths used to identify each transition are the center wavelengths for each of the bands listed in Table III of Judd[5] and may not exactly match the center wavelengths of the bands in Nd:SB″A: this is not of major importance since the Judd/Ofelt analysis is not concerned with the Stark multiplets that differ from host to host.

The most striking difference between the sets of data is the radical difference in the oscillator strength for the transition at 5760 Å. An examination of the reduced matrix elements for Nd^{3+} listed by Judd shows that the strength of this transition is most heavily affected by the parameter $\Omega_{2,\sigma}$. A linear term in the crystal field affects $\Omega_{2,\sigma}$ most strongly and any modeling of the nearest-neighbor environment must account for such a linear term.

Samples were prepared with a range of Nd^{3+} concentrations between $2.7\times10^{20}/cm^3$ and $1.7\times10^{21}/cm^3$. Ω parameters were calculated for each of these samples and the results are displayed graphically in Fig. 4.

Before accepting the values for the Ω parameters as generated by the least squares fit, the calculated Ω parameters must be placed back into the expression for oscillator strengths. This must then be compared to the oscillator strengths originally determined from the spectrum. Table II displays such a comparison for the classic work of Judd[5] on Nd^{3+} in chlorides and for the data discussed previously in Table I. In both cases, the column labeled P_{expt} are the oscillator strengths calculated directly from the spectra and P_{calc} are the oscillator strengths calculated from the Ω parameters generated by the least squares fit. As can be seen for both sets of data, the calculation favors the lines with the strongest

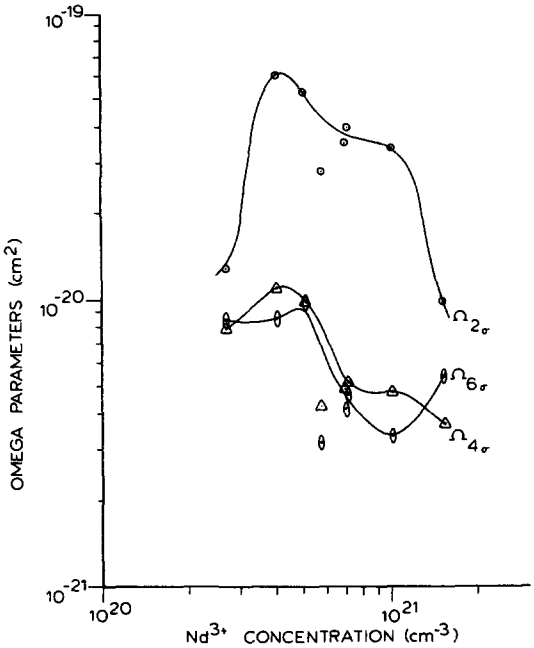

FIG. 4. Judd–Ofelt parameters (Ω parameters) for sigma polarization vs Nd^{3+} ion concentration.

oscillator strengths. Both sets of data show some lines with substantial percentage difference between P_{exp} and P_{calc}, with the Nd:SB″A data showing about the same quality of fit as the Nd:chloride data. Judd's analysis of the Ω parameters was derived from the spectra of thick crystals and as a result, several transitions too weak to be observed in the current work were included in Judd's least square fit. Additional data points for the Nd:SB″A data should lead to a better determination of the Ω parameters and a smaller RMS error in the calculated oscillator strengths.

Some uncertainty in the Ω parameters is expected from the error in measuring the areas under each line shape on the absorption spectra, however this has been found to be negligible. Typical uncertainties in area measurements are about 0.1 Å for lines at wavelengths shorter than 0.7 μ and about 0.2 Å for transitions at wavelengths longer than 0.7 μ. Although it would be difficult to analytically propagate this error through the calculation to determine the effect on the Ω parameters, a simple method that achieves the same result is to simply randomly scatter these errors through the measured areas before applying the least squares fit. We used this procedure for several of the samples and we observed that the effect on the Ω parameters is quite small (usually less than a few percent). It is interesting to note that the lines with large percentage errors between P_{expt} and P_{calc} are the same for both Judd's work and the current work. Further, it is noted that these lines are those for which $\Omega_{4,\sigma}$ and $\Omega_{6,\sigma}$ have the largest effect. It is expected that this error is inherent to the approximations made in the Judd/Ofelt analysis and not a function of the least squares fitting.

There was some concern that the anomalous oscillator strength for the line at 5760 Å might distort the calculations of $\Omega_{4,\sigma}$ and $\Omega_{6,\sigma}$. To study this possibility, this line was removed from the fitting and the Ω parameters recalculated for a representative sample. As shown in Table III, this change yields surprisingly little change in $\Omega_{4,\sigma}$ and $\Omega_{6,\sigma}$. Considering that $\Omega_{2,\sigma}$ will be strongly affected by the 5760 line, the moderate difference in $\Omega_{2,\sigma}$ calculated with the different data sets is expected and the fact that a reasonable value for $\Omega_{2,\sigma}$ can be calculated from the remaining weak lines is encouraging.

VI. QUALITATIVE MODEL FOR THE ORIGIN OF THE Ω PARAMETERS

Several pieces of information are known about the structure of exchanged SB″A or can be inferred with some certainty from the x-ray diffraction studies of earlier work. The first is that there must be both sodium and neodymium in the crystal and that it must coexist in the conduction plane. The second is that the nearest-neighbor environment cannot be

TABLE II. Oscillator strengths ($\times 10^{-6}$)—Calculated vs experimental.

	Judd–$NdCl_3$			Nd:SB″A ($n = 5\times10^{20}$ cm^{-3})		
Wavelength (Å)	P_{expt}	P_{calc}	% diff.	P_{expt}	P_{calc}	% diff.
3550	10.13	9.52	−6	13.0	11.9	−9
3800	0.04	0.05	2.5			
4188	0.06	0.08	33			
4320	0.43	0.38	−12	0.515	0.43	−17
4686	1.47	2.31	57	0.379	1.05	63
5171	5.48	6.58	20	6.63	7.35	9.8
5760	10.6	10.5	−0.9	47.9	47.79	−0.22
6256	0.20	0.39	95			
6710	0.78	0.83	6.4			
7390	9.84	8.88	−9.8	4.68	4.40	−6.0
7930	8.48	9.22	8.7	4.47	4.66	4.0
8678	2.02	3.02	49	1.27	1.46	13
rms error	0.73×10^{-6}			0.68×10^{-6}		
Ω_2	6.7×10^{-21} cm^2		$\Omega_{2,\sigma}$	51.9×10^{-21} cm^{-2}		
Ω_4	13.3×10^{-21} cm^2		$\Omega_{4,\sigma}$	9.73×10^{-21} cm^2		
Ω_6	27.3×10^{-21} cm^2		$\Omega_{6,\sigma}$	9.71×10^{-21} cm^2		

TABLE III. Ω parameters calculated with and without strong 5760 Å line for a sample with $n = 5\times10^{20}$ cm^{-3}.

	All lines	5760 Å removed
$\Omega_{2,\sigma}$	5.19×10^{-20} cm^2	3.99×10^{-20} cm^2
$\Omega_{4,\sigma}$	0.973×10^{-20} cm^2	1.02×10^{-20} cm^2
$\Omega_{6,\sigma}$	0.971×10^{-20} cm^2	0.983×10^{-20} cm^2

exactly that as described by Carillo–Cabrera as described in Sec. II since the structure so described exhibits inversion symmetry and is disallowed by the simple evidence that the crystal exhibits optical transitions. Finally, we recall that the oxygen ions in the conduction plane seem to be displaced by the introduction of gadolinium and presumably the position of the gadolinium or other rare earth is also capable of being displaced within a lattice of its nearest neighbors. Therefore, we may then qualitatively propose the following model for the nearest-neighbor environment as exchange progresses. Consider first the unexchanged conduction plane as shown in Fig. 5(a), showing the required vacant Beevers–Ross sites. By introducing a neodymium ion in Fig. 5(b) into one of the mid-oxygen sites, it might be expected that the sodium ions nearest to the mid-oxygen site would be replaced. The arrangement in Fig. 5(b) is still one which exhibits inversion symmetry and correspondingly has no oscillator strength. As the exchange process continues, this symmetric arrangement is not likely to last very long as neodymium ions begin to approach each other within a few unit cells. Therefore, one expects the oscillator strength to increase as the neodymium concentration increases.

At the opposite extreme, when exchange is essentially complete, the nearest-neighbor environment proposed by Carrillo–Cabrera is expected to be valid, which indicates a return to low oscillator strengths at high neodymium concentration. As can be seen from Fig. 4, this is essentially the behavior exhibited by the samples over the rather limited range of concentrations available in this work.

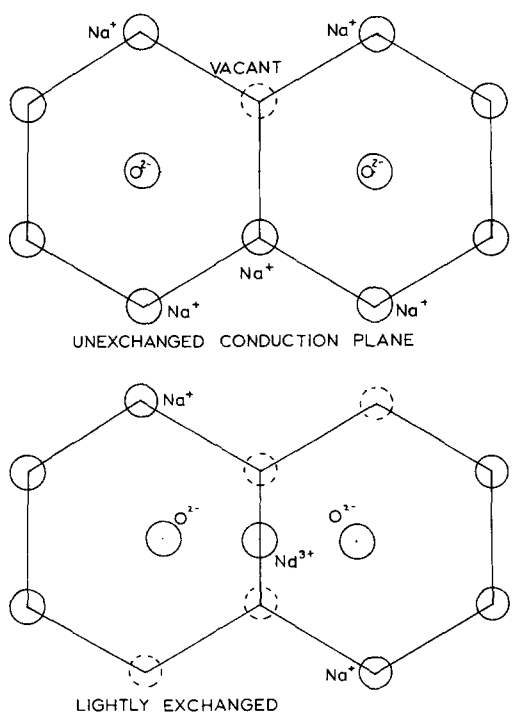

FIG. 5. Possible near-neighbor environments. In (a), an unexchanged sample is considered. In (b), a symmetric environment is considered for lightly exchanged samples.

VII. CALCULATION OF Ω PARAMETERS FROM POINT CHARGE MODELS

In principle, the even-order crystal field parameters may be experimentally determined from the energy level splitting of the Stark manifold for a given Russell–Saunders labeled level. Similarly, the odd-order crystal field parameters should also be attainable from the oscillator strengths of absorption lines. The crystal field parameters so obtained may then be compared to those calculated from a theoretical model. However, in practice, the odd order crystal field parameters are seldom obtained in this way since a list of oscillator strengths obtained by integration over a Stark multiplet is usually too short to uniquely determine all of the odd-order parameters. This is especially true for Nd:SB″A, which exhibits a low degree of symmetry near the Nd ion and therefore requires a complete set of the A_{tp} to completely specify the crystal field. Furthermore, it has long been recognized that a simple point charge model yields a poor fit between experiment and theory.[20] One example of a more elaborate point charge model improves the convergence of a point charge calculation by including contributions beyond the immediate rare-earth neighbors.[22] Of course, such a procedure requires a precise knowledge of neighboring ion positions out to a distance of over 10 Å from the rare earth ion; again a hopeless task for Nd:SB″A. Additionally, other more basic problems limit the quantitative use of the point charge model. These problems include poor knowledge of the radial integrals,[17] poor x-ray data of ion positions,[18] core electron shielding of the $4f^n$ electrons in the rare-earth ion,[15] and polarizability of the ions in the lattice surrounding the rare earth.[19] Burns[17] has presented a summary and analysis of several mechanisms that affect simple point charge crystal field calculations.

Given the aforementioned problems, one might be initially skeptical about the success of any point charge model. However, we anticipate that a comparison of the ratios of Ω parameters from experiment and theory for several proposed near-neighbor point charge environments may reveal the general character of the deviations from inversion symmetry. Several proposed deviations and their calculated Ω parameters will be examined and the qualitative effects of shielding discussed for each case.

By referring to Figs. 1 and 2 and to Ref. 10, the ion positions may be calculated for the near-neighbor oxygen ions in the spinel blocks above and below the conduction plane and for the oxygen ions in the conduction plane. As shown in Table IV, all positions are measured from the unperturbed Nd^{3+} ion, which is initially supposed to lie at the mid-oxygen site. All positions are listed in angstroms. From these data, the crystal field parameters $A_{t,p}$ are then calculated from

TABLE IV. Conduction plane ion positions in angstroms relative to the Nd^{3+} ion at the mid-oxygen site. Referring to Fig. 2, the origin is at the mid-oxygen site (2). The positive x direction points toward the bottom of Fig. 2 [in a line from site (2) to (3)] and the positive y direction points toward the right-hand side of Fig. 2 [in a line from site (2)–(5)].

Site	X coordinate	Y coordinate	Z coordinate
Nd(2)	0	0	0
O(5a)	0	−2.310	0
O(5b)	0	2.310	0
O(4a)	0.8294	−1.376	−2.223
O(4b)	−0.8292	−1.376	2.223
O(4c)	0.8294	1.376	−2.223
O(4d)	−0.8292	1.376	2.223
O(3a)	−1.624	0	−2.236
O(3b)	1.624	0	2.236

$$A_{tp} = (-1)^{p+1} \sum_i \frac{eq_i}{R_i^{t+1}} C^{(t)}_{-p}(\theta_i,\phi_i), \tag{19}$$

where the summation is over the near-neighbor point charges.

The first distortion considered is the addition of a single monovalent ion, presumably sodium, at some given distance from the neodymium ion. To simplify the calculation, we will consider each distortion independent of others and consequently, we first place the neodymium ion at the mid-oxygen site, with each oxygen at an equal distance from the neodymium. Therefore, the neodymium rests in a site which would exhibit inversion symmetry were it not for the addition of the monovalent ion. We may then remove all other ions from the calculation except the sodium and only its distance from the neodymium is important, not its angular orientation. The calculated Ω parameters are plotted vs ion distance in Fig. 6, using solid lines. The dashed lines are calculations made considering the polarization of the ligands and are discussed in Sec. VIII. Also plotted in this figure are the experimentally determined Ω parameters for a sample of concentration $5\times10^{20}/cm^3$. This ion concentration was selected as it shows the most severe effect of the linear field term and so is expected to be most easily modeled by the simple distortions to be considered here. Residual sodium is expected to be found at a site not immediately adjacent to the mid-oxygen site. As shown in Fig. 5, we expect sodium to lie at a distance of 4.30 Å from the neodymium and it can be seen from the plot of Fig. 6 that only the value calculated for $\Omega_{2,\sigma}$ compares closely with that determined expermentally. Most importantly, the calculated ratios for the Ω parameters do not fit well for virtually any reasonable spacing. As a first attempt, we then discard the possibility that sodium ions are solely responsible for the near-neighbor loss of inversion symmetry.

Since oxygen ions have been shown to move from their original positions in crystals that are totally exchanged, we then consider the possibility that a nonuniform distribution of sodium applies unequal forces to oxygen ions on either side of the neodymium. This might then place the two oxygen ions on either side of the neodymium at different distances from the neodymium. To model this effect, we then consider an arrangement with one oxygen ion in its unperturbed position at 2.81 Å from the neodymium. We then adjust the position of the other oxygen over a range of 0.5 from 2.8 Å from the neodymium along a line pointing to-

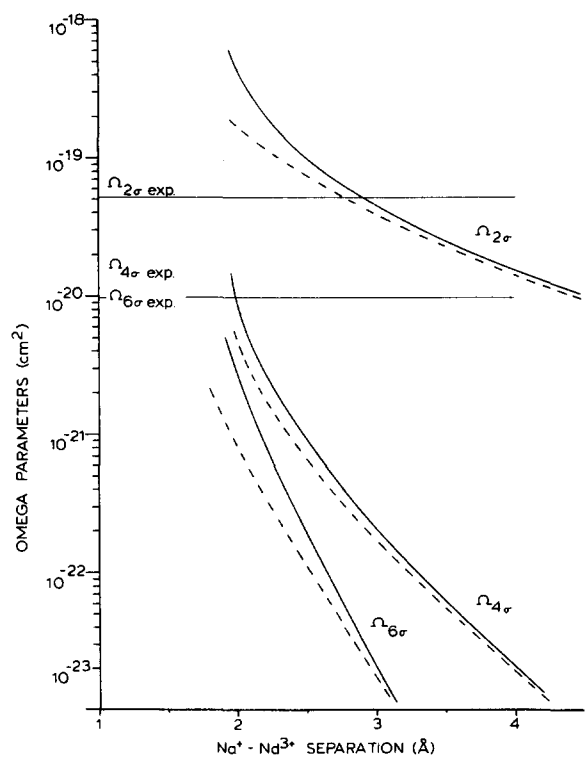

FIG. 6. Theoretical omega parameters for sigma polarization vs Na^+–Nd^{3+} ion separation. Solid lines are derived from a simple point charge model. Dashed lines include the effect of Na^+ polarizability of 1.35 a.u.[3]

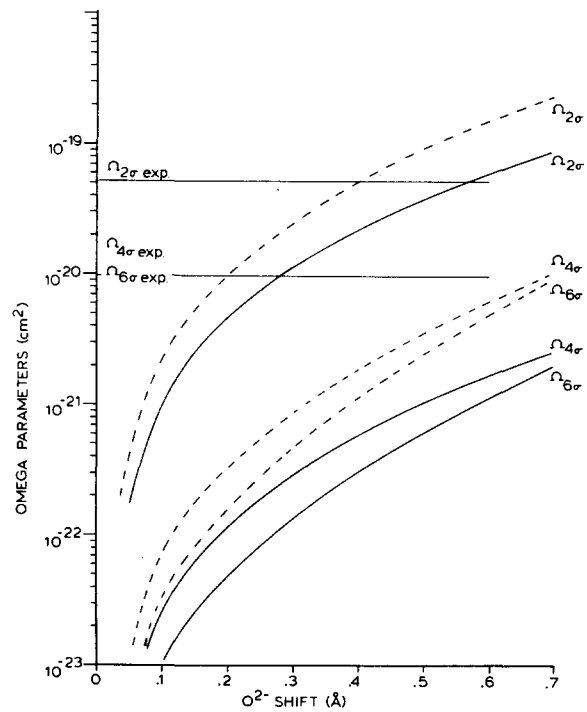

FIG. 7. Theoretical omega parameters for sigma polarization vs O^{2-} shift towards the near Beevers–Ross site measured from the unexchanged O^{2-} position. The opposing conduction plane oxygen is assumed to be at its unexchanged position of 2.81 Å from the mid-oxygen (Nd^{3+}) position. Dashed lines are for O^{2-} polarizability of 8.87 a.u.[3]

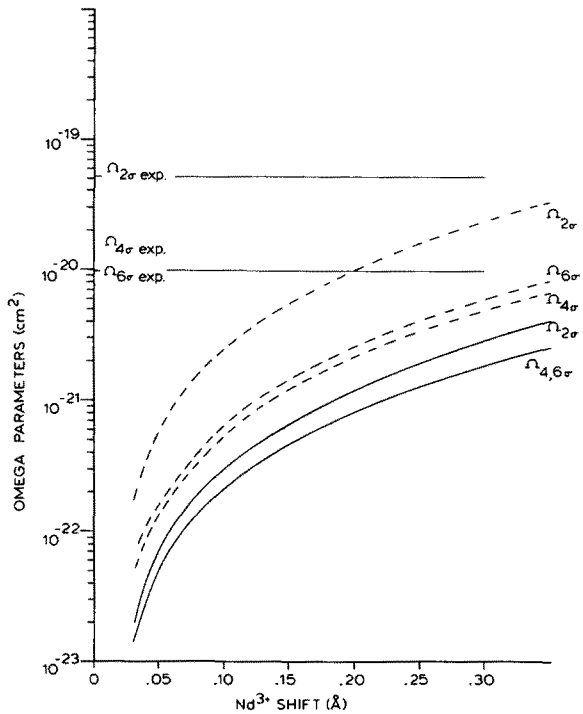

FIG. 8. Theoretical omega parameters for sigma polarization vs Nd^{3+} ion shift along a line connecting the undisturbed mid-plane O^{2-} sites. Conduction plane O^{2-} are assumed to be in their undistorted positions at 2.81 Å to either side of the mid-oxygen site. Dashed lines are for O^{2-} polarizability as per Fig. 7.

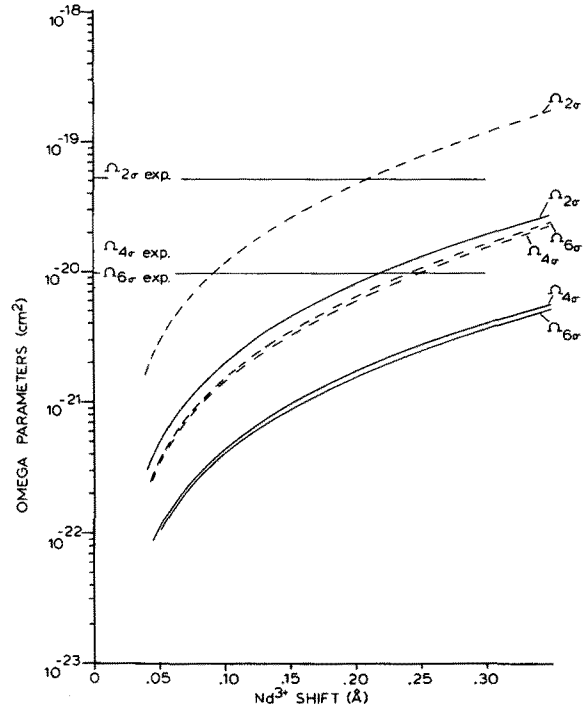

FIG. 9. Same plotting of omega parameters vs Nd^{3+} shift as displayed in Fig. 8 except that the conduction plane O^{2-} are assumed to be displaced inwards to a position 2.5 Å on either side of the mid-oxygen site.

ward the Beevers–Ross site.[12] As shown in Fig. 7 this fitting is somewhat better than that for sodium ion introduction only. Indeed, the $\Omega_{2,\sigma}$ parameter fits well for the size distortions believed to exist in the conduction plane. Further, the ratios of the calculated Ω parameters are closer to that observed in experiment for the proposed oxygen distortion than in the sodium ion model.

We next consider the possible shift of neodymium itself. As mentioned earlier, there is some "fuzziness" in the neodymium ion position. This might be expected if the neodymium ion sees a crystal field with one oxygen closer than another. For our final attempt at possible simple distortions, we simply take the symmetric environment suggested in the x-ray diffraction work[10] and apply a shift in the neodymium ion position along a line connecting the oxygen ions in the conduction plane. For this case, a computer run for all eight near-neighbor oxygen ions is needed. Results for this calculation are shown in Fig. 8 and show a relatively poor fit for even a large neodymium shift of 0.35 Å. However, if we pull the oxygen ions in toward the Nd^{3+} position by 0.3 Å (this type of distortion expected from Ref. 10) and again apply the Nd^{3+} distortion, as shown in Fig. 9, we see that the resultant Ω parameters are much more sensitive to this shift. The quality of the fit is remarkable when one considers that earlier workers have been content to be within an order of magnitude of the experimental value. However, it must be strongly noted that other experimenters did not have the artificial luxury of moving ions back and forth and were forced to live with ion positions determined by x-ray work. Note that the magnitudes of the distortions studied here are barely resolvable by x-ray diffraction. Further, it must be remembered that some justification for the neodymium shift must be proposed. For example, inclusion of an oxygen offset to induce the neodymium shift contributes to the Ω parameters as shown in Fig. 7 and indeed, makes the fitting worse. This is because the ratios $\Omega_{2\sigma}:\Omega_{4\sigma}$ and $\Omega_{2\sigma}:\Omega_{6\sigma}$ for oxygen displacement are larger than those for neodymium shift. Finally it should be apparent that the experimentally determined Ω parameters represent an average of several possible distortions that vary from site to site depending on the way sodium and neodymium are distributed over a range of several unit cells. It is easily shown by making a "game board" model of the conduction plane that, for a given neodymium concentration, several possible orientations exist for the remaining sodium and therefore, several possible induced distortions also exist.

VIII. CORRECTIONS TO THE POINT CHARGE MODEL OF THE CRYSTAL FIELD

Considering all of the above limitations for the point charge model, one might ask how it is possible for the point charge model to give useful results at all. Indeed, it might be suggested that the apparent success of the point charge model in the current work is simply coincidental. However, we will attempt to qualitatively show how polarizability and shielding may affect the Ω parameters in a way not inconsistent with the experimental results. Also, it is proposed that earlier work may have been affected by the sensitivity of the Ω parameters to ion position and the poor resolution of ion positions afforded by the x-ray data. No firm conclusions

may be reached however, until other rare-earth ions are exchanged into SB″A and the point charge analysis is repeated.

In Krupke's analysis[13] of rare-earth ions in Y_2O_3, concern was voiced over the inability to quantitatively introduce the effects of shielding on the calculations of the Ω parameters. Several authors have pointed out the possibility that shielding affects the lower order crystal field parameters more strongly than higher order parameters.[16] For example, the procedure of Lenander and Wong[16] was to determine how the point charge crystal field mixes higher order excited states into the closed shell wave functions. In so doing, they derived the polarization charge density represented by the perturbed closed shell electrons. The Coulomb interaction was then calculated between the polarized charge density and the charge density represented by the $4f$ wave functions. The perturbation was then expressed as a correction to the point charge crystal field parameters. The results showed that, while the sixth order crystal field term is essentially unaffected by shielding, the fourth order term will be reduced by 17% and the second order term reduced by 59%. Since Lenander and Wong performed their work for praseodymium and further, and were concerned only with even order crystal field terms, only qualitative projections may be made to neodymium in SB″A. We might expect that the $\Omega_{2,\sigma}$ parameter, which is the only term with a contribution from the first order crystal field A_{1p}, will be affected most severely. Further, less change is expected in $\Omega_{4,\sigma}$ and the least change of all is expected in $\Omega_{6,\sigma}$. This is essentially the effect required to improve the fitting for the theoretical calculations presented in the present work. Both the asymmetric oxygen distortion and the monovalent ion distortion show an excessively large value for the ratio $\Omega_{2\sigma}$:$\Omega_{4\sigma}$ and $\Omega_{4\sigma}$:$\Omega_{6\sigma}$. Shielding may indeed account for the observed discrepancy in these cases, but it is not expected to compensate for the enormous values for $\Omega_{2\sigma}$:$\Omega_{4\sigma}$ and $\Omega_{2\sigma}$:$\Omega_{6\sigma}$ seen in the monovalent ion distortion plot of Fig. 6. Therefore, we continue to discount the existence of monovalent sodium as the sole cause of the observed Ω parameters.

Hutchings and Ray[19] have considered the effect of the polarizabilty of the nearest-neighbor ions on the even-order crystal field parameters A_{tp}. Both dipole and quadrupole polarizabilities of chlorine ions in $PrCl_3$ were considered. From the results listed in their Table V, we see that the effect on the A_{tp} depends on whether both dipole and quadrupole contributions are included. If only dipole terms are considered, the A_{20} term is increased by nearly 60% whereas if quadrupole terms are also included, the net effect is a 30% reduction in A_{20}. Similar distortion exists for the higher order terms but the net effect on these terms is smaller than that for low order terms.

We may repeat these calculations for odd-order parameters by simply following the suggestion of Judd.[5] The technique of Hutchings and Ray[19] is to derive an expression for the effect on the crystal field parameters for arbitrary moments of all orders, with the moments aligned in an arbitrary direction. A much simpler approach is to consider dipole polarizability alone and assume that the induced dipoles will be aligned with the rare-earth ion. In this case, one may simply add a dipole moment term $u_i e(t+1)/R_i^{t+2}$ in place of the point charge term eq_i/R_i^{t+1} in expression (19). The dipole moment u_i is given by $\alpha Ze/R_i^2$ where α is the dipole polarizability of the ligand ion and $Z = 3$. Both the polarizability of Na^+ ions and O^{2-} ions are considered, the polarizabilities are those listed by Tessman *et al.*[21] Since the polarizability of O^{2-} is shown to be very dependent on the host lattice, we have chosen a value of the polarizability measured in Al_2O_3, since SB″A is essentially aluminum oxide. The polarizability so chosen is $1.31\,A^3$ and is converted to atomic units in the calculation. Similarly, the value selected for Na^+ is $0.2\,A^3$. The effect of polarization are indicated with dotted lines in Figs. 6–9. For the important O^{2-} and Nd^{3+} shift, the effect of polarizability is to simply raise all curves for the Ω parameters to higher values. Therefore, the same Ω parameters are achieved for less distortion. The calculated Ω parameters for a range of O^{2-} shift between 0.3 and 0.5 Å yield an acceptable fit to the experimental data. Further, from Figs. 8 and 9 it is quite interesting to note how little shift in the Nd^{3+} ion is now needed to yield radical changes in the Ω parameters.

Returning to the even-order crystal field, it can be seen from Ref. 19 that both polarizability and shielding as calculated in theoretical models do not yield orders of magnitude changes in simple point charge models and further, that the two effects may cancel each other somewhat. Yet enormous differences still exist between the experimental values and theoretical values for the products of even-order crystal field parameters and radial integrals. Hutchings and Ray[19] show that a one order of magnitude difference between experiment and theory is typical, and this will certainly not disappear if shielding is included. Therefore, we progress to the next possible source of error; the radial integrals.

Just as the inner core electrons may be distorted by the ligand field, the radial integrals of the $4f$ wave functions may expand from their free-ion values. This is caused by the penetration of the ligand wave functions into the rare-earth ions and consequent shielding of the rare-earth $4f$ wave functions from the rare-earth nuclear charge. Using the curves displayed by Hutchings and Ray[19] representing the Hartree radial wave functions for the chlorine ligand field, Burns[17] derived a simplified form for the charge density represented by the ligand ions. Burns then performed essentially the same calculation as Lenander and Wong[16] to calculate a perturbed potential energy for the $4f$ electron. New values for the radial integrals are then calculated using this perturbed potential. The expansion of the radial integrals is essentially zero for $\langle 4f|r^2|4f\rangle$, 12% larger for $\langle 4f|r^4|4f\rangle$, and 36% larger for $\langle 4f|r^6|4f\rangle$. However, from Judd, we see that these integrals are only used in calculating the contribution of higher order configurations on the Ω parameters and that the real integrals of importance are those of the form $\langle 4f|r^t|5d\rangle$. Krupke[13] implies that he has calculated the perturbations to these integrals and finds them essentially unchanged except for $\langle 4f|r|5d\rangle$, which he claims "shows a marked decrease with radial expansion due to the relatively greater contribution of negative regions of the $5d$ wave function." However, no further details are given in the referenced work so the size of the errors in the radial integrals cannot be readily determined.

IX. CONCLUSION

We therefore conclude that the observed sigma polarized absorption spectra for Nd:SB″A can be explained to first order by using a point charge model for the near-neighbor crystal field that includes the possibility for a slight shift in the position of Nd^{3+} and O^{2-} conduction plane ions. The shift is believed to be induced by the nonuniform distribution of sodium ions in each unit cell. Improved results are obtained by including a simple model for the polarizability of the near neighbors. Although the uncertainty in the position of the crystal field ions makes a properly converged point charge analysis impractical, the authors believe that one may qualitatively choose certain types of ion dislocations to be responsible for the observed line strengths.

ACKNOWLEDGMENTS

The authors would like to thank L. Salmon of the Department of Materials Science for performing some of the crystal growth, H. Dai for assembling the laser spectrophotometer, and especially Professor E. Y. Wong of the UCLA Department of Physics for many hours of invaluable assistance and discussion. This research was supported in part by a grant from the U. S. Office of Naval Research.

[1]G. C. Farrington and B. Dunn, Solid State Ion. **7**, 267 (1982).
[2]B. Dunn and G. C. Farrington, Solid State Ion. **9/10**, 223 (1983).
[3]M. Jansen *et al.*, Opt. Lett. **9**, 119 (1984).
[4]B. R. Judd, J. Chem. Phys. **70**, 4830 (1979).
[5]B. R. Judd, Phys. Rev. **127**, 750 (1962).
[6]G. S. Ofelt, J. Chem. Phys. **37**, 511 (1962).
[7]T. S. Lomheim and L. G. DeShazer, J. Appl. Phys. **49**, 5517 (1978).
[8]T. S. Lomheim and L. G. DeShazer, Phys. Rev. B **20**, 4343 (1979).
[9]J. P. Boilot, G. Collin, Ph. Colomban, and R. Comes, Phys. Rev. B **22**, 5912 (1981).
[10]W. Carrillo-Cabrera, J. O. Thomas, and G. C. Farrington, Solid State Ion. **9/10**, 245 (1983).
[11]W. L. Roth, R. E. Benenson, V. K. Tikku, J. L. Briant, and B. Dunn, G. E. Corporate Research and Development Report #81CRD185, 1981.
[12]J. O. Thomas (private communication).
[13]W. F. Krupke, Phys. Rev. **145**, 325 (1966).
[14]W. F. Krupke, IEEE J. Quant. Electron. **10**, 450 (1974).
[15]W. F. Krupke, IEEE J. Quant. Electron. **7**, 153 (1971).
[16]C. J. Lenander and E. Y. Wong, J. Chem. Phys. **38**, 2750 (1963).
[17]G. Burns, J. Chem. Phys. **42**, 377 (1965).
[18]W. H. Zachariasen, J. Chem. Phys. **16**, 254 (1948).
[19]M. T. Hutchings and D. K. Ray, Proc. Phys. Soc. **81**, 663 (1963).
[20]M. T. Hutchings and W. P. Wolf, J. Chem. Phys. **41**, 617 (1964).
[21]J. R. Tessman, A. H. Kahn, and W. Shockley, Phys. Rev. **92**, 890 (1953).
[22]M. Faucher and P. Caro, J. Chem. Phys. **66**, 1273 (1977).